THE JOURNAL OF PHYSICAL CHEMISTRY C
A JOURNAL OF THE AMERICAN CHEMICAL SOCIETY

pubs.acs.org/JPCC

Perspective

Corrosion of Electrochemical Energy Materials: Stability Analyses Beyond Pourbaix Diagrams

Alexandra Zagalskaya,[§] Payal Chaudhary,[§] and Vitaly Alexandrov*

Cite This: https://doi.org/10.1021/acs.jpcc.3c01727

Read Online

ACCESS | Metrics & More | Article Recommendations

ABSTRACT: Since their first appearance, electrode potential/solution pH charts (Pourbaix diagrams) have served as a general framework for the analysis of material corrosion in aqueous solutions. Their utility in describing electrochemical stability of materials is rooted in the equilibrium thermodynamics based formalism. Electrochemical energy systems, however, do not always operate under thermodynamic equilibrium conditions, and corrosion itself is an inherently irreversible interfacial process. In this Perspective, we highlight a number of representative studies drawn primarily from (photo)electrocatalysis research and aimed to account for the effects of potentiodynamic polarization and transient dissolution, interfacial electrochemical reactions, formation and stability of metastable phases, strain-induced corrosion, as well as the kinetics of dissolution and phase transformations. Some theoretical approaches that can help disentangle corrosion mechanisms under conditions relevant to electrochemical energy conversion applications are briefly discussed. We also advocate for more research efforts directed at the basic science of electrochemical corrosion that has long been deemed as a not "fancy" topic.

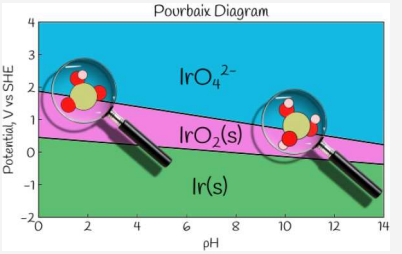

INTRODUCTION

Metal corrosion has been a serious impediment to the development of human civilization. Pliny the Elder (AD 23–79), the early Roman Empire's philosopher and army commander, wrote extensively about metallurgy in his encyclopedic treatise "Natural History". A special place was held for iron due to its use for weaponry, where the corroded metal is called *"ferrum corrumpitur"* (spoiled iron). It was believed that corrosion of metals is the punishment of the gods. Since then, the humanity has made tremendous strides to remove the pall of superstitions and adopt the methods of science to advance our understanding of metal corrosion. However, the center of gravity in our corrosion research has been disproportionately displaced toward empirical trial-and-error; not without astonishing successes, of course. One of the celebrated examples of such Edisonian approach in corrosion science is the advent of rust-resistant (stainless) steels in 1913 by Harry Brearley truly revolutionizing manufacturing in the 20th century. Another example is cathodic protection discovered by Humphry Davy and Michael Faraday in the first half of the 19th century, but finding practical realization only some 100 years afterward.

An important step in our fundamental understanding of metal corrosion in aqueous environments has been the invention of electrode potential/solution pH diagrams published by Marcel Pourbaix in 1945 as his doctoral thesis.[1] These electrochemical phase diagrams derived from the laws of equilibrium thermodynamics have become a major framework for the treatment of corrosion problems ever since. In recent years with the widespread application of electrochemical energy storage and conversion technologies, Pourbaix diagrams have been extensively utilized to rationalize and predict the corrosion behavior of energy materials. Furthermore, the launch of the Materials Genome Initiative in 2011 has helped to intensify community efforts in automating the construction of such thermodynamic diagrams. This has led to the emergence of so-called computational Pourbaix diagrams now available as part of the Materials Project.[2−4] This approach has become an indispensable theoretical tool to enable rapid thermodynamic analyses of materials corrosion that are now routinely accompanying high-throughput screening investigations of electrochemical energy materials. Originally, Pourbaix diagrams were not designed to consider out-of-equilibrium systems. Although useful as the first step in the stability analysis of energy materials, the pervasive application of such thermodynamic diagrams may lead to the wrong impression that such an analysis is sufficient. Moreover, Pourbaix diagrams do not provide critical details about corrosion mechanisms, how the transitions between equilibrium phases occur when electrode potential and local pH are changed, and how these transitions are manifested in materials instability.

Received: March 14, 2023
Revised: June 6, 2023

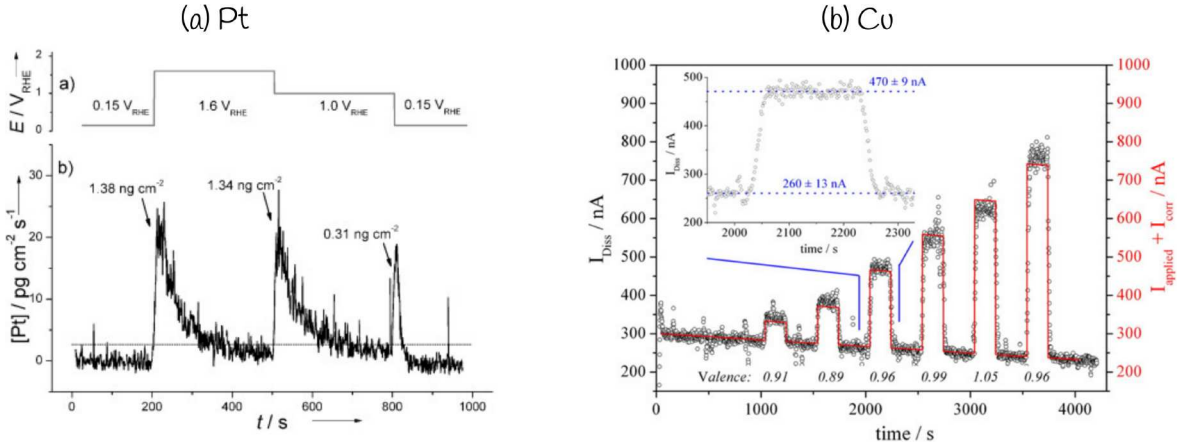

Figure 1. (a) Pt dissolution profile under steady-state conditions with potential holds at +0.15, +1.6, +1.0, and +0.15 V_{RHE}. The dotted line indicates the detection limit for the measurement. Reprinted with permission from ref 8. Copyright 2012 Wiley-VCH. (b) Cu dissolution profile (I_{Diss}, hollow spheres, left axis) and overlaid sum of applied current and corrosion current ($I_{applied} + I_{corr}$, red line, right axis). The inset shows the magnified region between 1950 and 2330 s with a linear approximation of the plateau values for the baseline and during galvanostatically applied current (100 nA). Reprinted with permission from ref 14. Copyright 2011 Elsevier.

The goal of this Perspective is to draw attention to several aspects for which analysis is not readily available from standard Pourbaix diagrams but are important for a more complete description of corrosion behavior. In particular, we discuss the role of potentiodynamic polarization of the electrodes resulting in transient dissolution, formation and stability of metastable phases, strain-induced electrochemical corrosion, different electrocatalytic reaction pathways at the interface destabilizing the catalyst, and kinetic control. We note that all of these factors may simultaneously contribute to materials instability to varying degrees depending on the material and working conditions. It is, however, instructive to discuss these factors separately. We also outline some theoretical approaches that can be employed to address these aspects in light of materials instability. Here, we skip the description of the formalism underlying the construction of Pourbaix diagrams and refer the reader to the available literature.[5−7]

DISCUSSION

Potentiodynamic Conditions and Transient Dissolution. One tacit assumption of any theoretical analysis based on Pourbaix diagrams is that thermodynamic equilibrium is reached. This also assumes that even if the electrode potential changes, it does so in a quasi-equilibrium fashion. This is not always the case in practice due to the transient operating conditions of many energy conversion devices including fuel cells and electrolyzers.[8−12] Moreover, the cycling between reducing and oxidizing potentials can be deliberately employed to steer reactivity of electrocatalysts.[13] It was demonstrated, however, that such potential fluctuations may result in transient dissolution, i.e., dissolution during a transition between two thermodynamically stable phases. What is important is that transient dissolution may substantially exceed dissolution under steady-state conditions.[8] It was also shown that, depending on the metal, transient dissolution could be more pronounced under either cathodic (negative-going) or anodic (positive-going) potential scans.[10] We still do not quite understand the mechanistic reasons behind these observations.

For example, previous experiments using electrochemical online inductively coupled plasma mass spectrometry (ICP-MS) provided real-time data on Pt dissolution as a function of dynamically changing electrode potential.[8] These voltage cycling experiments were aimed at mimicking the startup-shutdown cycles of an automative fuel cell in which Pt catalyzes the oxygen reduction reaction (ORR). Crucially, it was revealed that the most severe Pt dissolution occurs during the cathodic potential sweeps, while the anodic potential scans resulted in much lower Pt dissolution rates. It was proposed that the oxidation of the Pt surface is complete at about U = 1.15 V_{RHE}, while a further increase in the potential leads to the formation of a subsurface oxide of unknown nature. It was hypothesized that the observed reductive dissolution of Pt is related to the subsurface oxide.

The observed transient nature of Pt dissolution can be contrasted with the case of Cu that exhibits time-independent metal dissolution.[14] Figure 1 demonstrates the distinctive behavior of Pt and Cu dissolution as revealed by the same experimental techniques. It can be clearly seen from the figure that the rate of Pt dissolution decreases significantly during the first 200 s as a response to a potential perturbation. In contrast, an excellent agreement between Cu dissolution and applied current is observed with sharp transitions between the open-circuit potential (OCP) measurements and applied currents as seen from Figure 1.

A recent computational study has attempted to reveal the reaction mechanism of Pt dissolution and the nature of the subsurface oxide formed during potential cycling to explain transient dissolution observed in experiments.[11] Based on DFT calculations under constant-potential conditions in conjunction with the genetic algorithm of global structural optimization, the following Pt dissolution mechanism was proposed:

$$\text{anodic sweep: } 3Pt + 4H_2O \rightarrow Pt_3O_4^s + 8(H^+ + e^-) \quad (1)$$

$$\text{cathodic sweep: } Pt_3O_4^s + 8H^+ + 6e^- \rightarrow [Pt(H_2O)_4]^{2+} + 2Pt \quad (2)$$

Specifically, during the anodic potential scan (eq 1), the Pt surface is oxidized undergoing a surface reconstruction at U > 1.1 V_{RHE} to produce a surface oxide $Pt_3O_4^s$ consisting of corner-sharing square planar PtO_4 motifs. During the cathodic scan (eq 2), the newly formed surface oxide is first reduced to a Pt hydroxide at U = 1.0 V_{RHE} and pH = 1, which is subsequently

https://doi.org/10.1021/acs.jpcc.3c01727
J. Phys. Chem. C XXXX, XXX, XXX−XXX

reduced and dissolves as $[Pt(H_2O)_4]^{2+}$. Despite getting very insightful results, the study does not consider some other factors that might play a role, such as kinetics of phase transformations and lattice strains generated during potential cycling. These aspects will be discussed in the next sections.

While static DFT calculations can provide extremely valuable insights into the stability of energy materials including via DFT-calculated Pourbaix diagrams, they do suffer from a number of shortcomings especially when it comes to describing the time-dependent evolution of reacting interfaces. In this regard, the methods based on reactive force-field (ReaxFF) empirical interatomic potentials can reach much larger simulation scales.[15] One example of the application of the ReaxFF formalism to corrosion is the study of Pt surface degradation in which the oxidation of 2−4 nm Pt particles was simulated employing a ReaxFF within a grand-canonical Monte Carlo scheme.[16] The constructed potential-dependent phase diagrams suggested that surface oxide structures should be stable between 0.8 and 1.1 V_{SHE}, but should form anionic subunits of Pt_6O_8 stoichiometry beyond 1.1 V_{SHE}. Detachment of such Pt_6O_8 clusters from a fully oxidized particle into solution was also modeled, suggesting its important role in Pt degradation. These results are in good agreement with predictions from DFT simulations.[11,16] ReaxFF models are thus capable of pinpointing a multitude of metastable structures formed during the oxidation of metal surfaces,[16,17] as well as providing insights into transient behavior.[18] These studies demonstrate the feasibility of a well-developed ReaxFF model for investigations of catalyst degradation phenomena over a wider range of structural configurations than is accessible to DFT.

Another approach to overcoming the sampling limitations of DFT is to combine it with machine learning (ML) approaches. Such ML-assisted first-principles simulations may help elucidate the atomistic details of dynamically evolving electrochemical interfaces under reaction conditions.[19−24] For example, in a recent work combining microscopy, spectroscopy and accelerated ML molecular dynamics a detailed atomistic picture of dynamic surface restructuring of Pd deposited on Ag was revealed.[20] It was demonstrated in simulations and confirmed by surface science experiments that in contrast to the thermodynamically favored states, where Pd is dispersed in the Ag bulk, nontrivial metastable structures should prevail at mild temperatures. Critically, the observed restructuring behavior has a profound effect on the catalytic performance, as activation of the catalyst is enabled by surface metastable states. It should be noted that the study focused on bare alloy interfaces, simplifying the overall treatment due to the absence of electrical double layer effects arising in aqueous electrocatalysis.

Unfortunately, the application of DFT-ML methods to understand the mechanisms of electrochemical corrosion in aqueous environments is still quite rare.[23−27] Nevertheless, we believe that a combination of DFT and ML tools can be extremely helpful in tackling complex corrosion problems. Recent advances in deep ML including the approaches based on Boltzmann generators[28] can significantly help with sampling of equilibrium states. Moreover, these methods can avoid the need to manually specify reaction coordinates to examine transitions between metastable states that is necessary for many enhanced sampling methods such as metadynamics and umbrella sampling.[29]

In an attempt to generalize the results on Pt transient dissolution behavior discussed above, a recent investigation analyzed electrochemical dissolution of a series of representative 3*d*, 4*d*, and 5*d* transition metals under potentiodynamic conditions in both acidic and alkaline media.[10] It was found that during the anodic potential scans leading to oxide formation at η = 200 mV in base, all of the investigated metals underwent transient dissolution with the extent of dissolution increasing within each *d*-shell. However, during the reduction of the formed oxide layers, dissolution behavior was found to differ considerably. In particular, transient reductive dissolution was observed in the case of Rh, Ir, Pt, and Ru, while no dissolution was detected for 3*d* metals (Fe, Co, and Cu). In acidic media, 3*d* metals were excluded from the analysis due to their severe corrosion.

It was also shown that transient anodic dissolution correlates reasonably well with metal cohesion energy (M−M bond strength), while transient cathodic dissolution correlates with oxygen adsorption energy (M−O bond strength). Thus, it turned out that even such basic descriptors can be employed to explain dissolution trends across transition metals fairly well. Nevertheless, building a more quantitative theory capable of describing both steady-state and transient dissolution regimes would require more detailed atomistic information. For example, it was recently revealed by combining experiments with DFT simulations that the marked difference in the anodic dissolution of Pt(111) and Pt(100) upon oxidation originates from the different atomic structures of the initial oxide.[30] This in turn leads to different Pt extraction mechanisms affecting the process reversibility and materials stability.

On the other hand, the formation of an oxide layer during metal oxidation may in fact be beneficial for materials stability. A well-known example is stainless steels, in which the addition of alloying elements such as Cr or Mo leads to the formation of protective passive films improving corrosion resistance. Novel materials design strategies such as the use of high-entropy alloys may even result in superior corrosion-resistant properties compared with conventional alloys.[31,32] Overall, these investigations showcase the significance of atomic-scale insights into the intricate interplay between different interfacial subprocesses such as surface oxidation, restructuring, and metal dissolution to explain time-dependent corrosion behavior beyond the Pourbaix diagram analysis. These studies also enrich our understanding of how to control dynamic interfacial behavior to steer catalytic activity without significant compromises in electrode stability.

Strain-Induced Electrochemical Corrosion. Lattice strain is an important factor that influences the corrosion behavior of energy materials. In electrocatalysis, strain engineering has emerged as an efficient strategy to tune electrocatalytic activity.[33−38] But even if the strain is not deliberately exploited to enhance activity, electrochemical processes involving oxidation or reduction of the surface atoms and adsorption of reaction intermediates will always induce local lattice strain.[39,40] This in turn will affect not only catalytic activity but also materials stability since strain modifies the electronic structure of the surface sites. Such strain effects can be pronounced even for the most noble metal electrodes, such as Pt and Pd. For instance, electrochemically driven incorporation of hydrogen into the bulk Pd nanocrystal is known to induce severe Pd lattice expansion causing a phase transition.[41] In the case of Pt, which is one of the best catalysts for the hydrogen evolution reaction, surface Pt hydride structures of several monolayers may form thereby playing an important role in activity and cathodic corrosion of Pt.[42−44] This will introduce significant lattice strains

https://doi.org/10.1021/acs.jpcc.3c01727
J. Phys. Chem. C XXXX, XXX, XXX−XXX

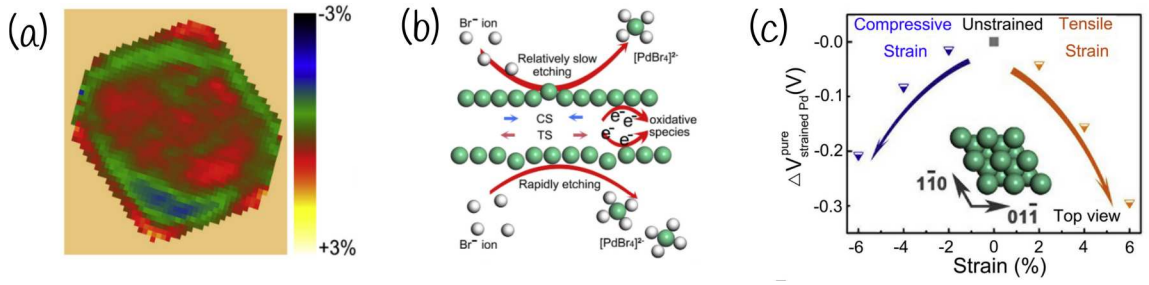

Figure 2. (a) Strain map of the Pt@Pd octahedron before corrosion. (b) Comparison of the etching under compressive and tensile strain. (c) Calculated dissolution electrode potential difference between Pd(111) slabs and the unstrained Pd(111) slab. Reprinted with permission from ref 39. Copyright 2020 Cell Press.

that should cause surface reconstruction and eventual Pt detachment to solution.[44,45]

A recent investigation focused on analyzing the relationship between strain and corrosion in Pd@Pt core−shell octahedral nanoparticles.[39] This system exhibits one of the best electrocatalytic activities toward the ORR. The study revealed that both the static local strain and the evolving curvature synergistically control the nanoscale corrosion kinetics. In particular, it was determined that corrosion starts from defects in the corners and terrace due to accumulated strain of the Pd and Pt lattice mismatch. For example, Figure 2a shows the distribution of strain across the 37 nm octahedron before corrosion covering the range from −3% compressive strain to +3% tensile strain. The time-sequential transmission electron microscopy (TEM) demonstrated that the etching process starts from a corner defect and propagates to the center of the nanoparticle. It was also shown that small strain (either compressive or tensile) always has a lower and large strain has a higher etching rate. Also, tensile strain was determined to cause faster etching than compressively strained samples (see Figure 2b). To complement these experimental observations, DFT simulations were undertaken. Figure 2c shows the calculated dissolution potential difference between strained Pd(111) slabs and unstrained Pd(111) slab. It is seen that both compressive and tensile strain should promote the etching process with tensile strain leading to a more pronounced dependence indicating easier etching in agreement with experiments.

It was previously demonstrated on the example of single crystals and nanoparticles that the electrochemical strain is a direct consequence of charge adsorption processes.[40,46,47] For example, it was measured that the lattice constant is minimum at the potential of zero total charge (pztc) and increases upon adsorption of positively or negatively charged species.[40] Moreover, a robust linear relationship between the relative variation of the lattice constant and the measured charge transfer for both potential sweep directions from the pztc was determined upon electrochemical monitoring of adsorption on Pt electrodes. This suggests that experimentally measurable lattice strain could serve as a structural descriptor of adsorption and catalytic trends.[48]

In a recent DFT investigation the role of strain was analyzed for the case of the lattice oxygen mechanism (LOM) of the oxygen evolution reaction (OER) across a series of perovskite oxides.[49] This mechanism, to be discussed in the next section, is often associated with surface instability and metal dissolution during the OER.[50,51] Specifically, it was shown using DFT calculated free energy diagrams that lattice oxygen involvement can explain the improved OER and ORR activities of compressively strained $LaNiO_3$.

In addition, we point out that electrochemical dissolution driven by strain could also be important in the context of transient dissolution discussed in the previous section. This is because the changes in electrode potential, depending on the scanning rate, could be much faster than the structural modifications and (electro)chemical transformations induced by potential fluctuations. This will unavoidably lead to the strain accumulation affecting the materials stability. The interplay between potential changes, induced strains, and corrosion of (photo)electrocatalysts is not well understood. Overall, theoretical modeling of catalyst dissolution and surface restructuring induced by strain could help decouple the role of strain from other contributions and, thus, provide useful insights into corrosion behavior.

Interfacial Electrochemical Reactions. It is established that the stability of the same electrode material may strongly depend on the nature of the interfacial electrochemical reaction. For instance, it was demonstrated on the example of Pt electrodes that continuous Pt dissolution occurs during the OER, limited dissolution takes place during the CO oxidation reaction, and no dissolution was observed during the ORR.[52] But even under similar experimental conditions, electrochemical energy materials may undergo multiple competing interfacial processes that have different repercussions for materials stability. Therefore, atomic-scale knowledge of such reaction pathways and their role in electrochemical stability depending on conditions such as solution pH and electrode potential is important for developing a predictive understanding of materials (in)stability.

One example is the OER over metal-oxide electrocatalysts that can proceed via a number of reaction pathways. In the past, the so-called adsorbate evolving mechanism (AEM) has become the classical mechanism of the OER widely analyzed in literature. The AEM pathway is conventionally divided into four elementary proton-coupled electron transfer steps involving oxygen intermediates *OH, *O, and *OOH as follows:

$$\square^* + H_2O \rightarrow HO^* + e^- + H^+ \quad (3)$$

$$HO^* \rightarrow O^* + e^- + H^+ \quad (4)$$

$$H_2O + O^* \rightarrow HOO^* + e^- + H^+ \quad (5)$$

$$HOO^* \rightarrow O_2(g) + e^- + H^+ + \square^* \quad (6)$$

The OER thermodynamics is most commonly studied using the computational hydrogen electrode approach.[53,54] The method enables an evaluation of the thermodynamic overpotential for the overall OER using DFT calculations as

https://doi.org/10.1021/acs.jpcc.3c01727
J. Phys. Chem. C XXXX, XXX, XXX−XXX

$$\eta_{OER} = \max[\Delta G_1, \Delta G_2, \Delta G_3, \Delta G_4]/e - 1.23V \quad (7)$$

where ΔG_i (i = 1, 2, 3, 4) are the calculated free energies of the AEM reaction steps and 1.23 V is the equilibrium potential of water splitting. A distinctive feature of the AEM is that the reaction occurs over the same surface transition-metal center, exemplifying a cationic redox reaction.

Previously, alternative OER pathways have been proposed including the so-called LOM.[49,55−62] The metal oxides capable of lattice oxygen redox chemistry were found to exhibit pH-dependent OER activity on the reversible hydrogen electrode scale. This indicates nonconcerted proton−electron transfers during the OER unlike the conventional AEM. Figure 3 depicts

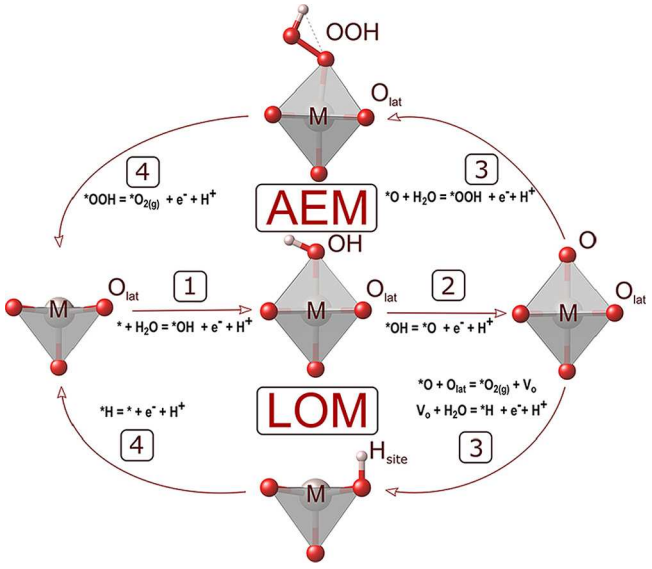

Figure 3. Schematic representation of the AEM and LOM of the OER over the rutile MO_2(110) surface. Reprinted with permission from ref 61. Copyright 2020 American Chemical Society.

AEM and LOM reaction pathways on the rutile MO_2(110) surface structure. Here, we refer to a large body of previous work discussing the role of lattice oxygen activation in the OER and ways to enhance OER activity via LOM.[60,63,64]

What is far less understood, however, is the role of LOM in the electrochemical stability of catalysts. When lattice oxygen is involved in the electrochemical generation of O_2 product from water, it leads to the breaking of lattice M−O bonds, formation of structural oxygen vacancies and overall destabilization of the catalyst structure. On the basis of a general thermodynamic analysis it was revealed that metal-oxide dissolution and LOM are universally linked being both triggered during the OER.[58] However, the microscopic details remain largely unclear. Experimentally, it was shown that LOM can indeed have a significant impact on electrochemical stability, but it depends on the system. For example, by using various experimental techniques such as isotope labeling with atom probe tomography and electrochemical mass spectrometry, it was demonstrated that most of the Ir-based alloys and mixed oxides,[50,51] sputtered Ru oxides,[56] as well as many non-noble perovskites,[59,65] transform to amorphous or hydrous oxides evolving oxygen from the lattice. In the case of the $SrIrO_3$ OER electrocatalyst, amorphization was found to be triggered by the lattice oxygen activation that leads to coupled Sr^{2+} and O^{2-} diffusion at the oxide−electrolyte interface.[66] This surface restructuring process results in the formation of a highly disordered, amorphous film composed of $Ir^{4+}O_6$ octahedra with Sr^{2+}-Ir^{3+} residue. The final structure was found to be more disordered than the electrochemically or thermally grown amorphous IrO_x.

On the other hand, no lattice participation in the OER was observed for Pt[67] and thermally prepared RuO_2.[68] In the case of $LaNiO_3$, although pronounced involvement of lattice oxygen in the OER was detected[69] in agreement with theoretical predictions,[49] the surface largely remained crystalline and in the perovskite phase after the OER.

Another recent investigation focused on the processes occurring at the surfaces of calcined and uncalcined IrO_2 nanoparticles during water electrolysis.[70] It was found that the mechanism of the OER should change at higher potentials, which impacts the durability of the catalyst. Specifically, it was determined that calcined IrO_2, after removal of lattice oxygen, exhibited stronger Ir−Ir interaction at OER potentials above 1.5 V compared to uncalcined IrO_2 leading to the increased dissolution stability of the IrO_2 catalyst after calcination. This outcome was attributed to the formation of a periodic Ir−O−Ir structure in calcined IrO_2 after oxygen removal, resulting in lower oxidation state of Ir at higher potentials. These results were further supported by *ab initio* molecular dynamics (AIMD)-based simulations that showed a significantly increased energy barrier for Ir dissolution from reduced IrO_2, with the first transition from Ir(III) to Ir(IV) contributing the most to the dissolution barrier.

A subsequent DFT modeling study focused on comparing interfacial reoxidation dynamics for the rutile(110) surface of RuO_2 and IrO_2 as a response to the OER proceeding via the LOM.[71] It was found that these oxides display qualitatively different reoxidation behavior, which has important implications for their electrochemical stability. In particular, it was observed that in contrast to IrO_2(110), which is forming highly stable low oxidation state Ir(III) species as a result of LOM, Ru species at RuO_2(110) undergo facile reoxidation by solution water. This should in turn facilitate the formation of high Ru oxidation state intermediates, promoting metal dissolution.

In another recent experimental study, the OER activity and stability of a series of complex perovskite catalysts were analyzed in a wide range of solution pH (7−14).[72] It was demonstrated that different mechanisms of the OER (AEM and LOM) are predominant in different pH regions. Interestingly, it was revealed that most investigated perovskites exhibit the greatest stability at higher pH levels where LOM appears to dominate over the classical AEM mechanism, suggesting formation of a dynamically stable surface.

The examples discussed above demonstrate that the involvement of the LOM in the OER may have a complicated effect on catalyst stability. It was pointed out in many previous studies that surface reconstruction during the OER is not synonymous to electrochemical instability.[72−74] In fact, a dynamic process of metal dissolution and redeposition back to the surface leading to a modified interface with often improved OER activity and stable performance can be considered as "dynamic stability". Therefore, there is certainly a need to better understand atomistic details of the overall OER process including lattice oxygen redox from both thermodynamic and kinetic points of view and how it affects electrochemical stability of electrocatalysts.

Formation and Stability of Metastable Phases. (Photo)electrochemical processes may lead to the destabiliza-

https://doi.org/10.1021/acs.jpcc.3c01727
J. Phys. Chem. C XXXX, XXX, XXX−XXX

tion of thermodynamically stable materials and facilitate the formation of metastable phases. Depending on working conditions, these metastable phases may be short- or long-lived and even define the overall interfacial activity and stability.[12,75−77] Thus, in some cases, material interfaces can be in constant state of dynamic metastability making it challenging to analyze their properties based solely on equilibrium Pourbaix diagrams. Metastable phases may exhibit catalytic activity much higher than that of their thermodynamically stable parent structures, albeit often at the expense of their stability. This has led to increasing efforts to develop metastable materials for electrocatalytic energy conversion applications.[78]

Electrochemical stability of metastable materials has started attracting attention from a theoretical perspective relatively recently. One proposed approach is the extension of Pourbaix diagrams to include the relative Gibbs free energy of metastable materials as a function of solution pH, electrode potential, temperature and bulk concentration of aqueous species.[75] Since metastable phases cannot lead to thermodynamically favorable redox reactions, their Gibbs free energy (ΔG_{pbx}) is taken with respect to the Pourbaix stable domains as a function of pH and potential, and thus, $\Delta G_{pbx} = 0$ corresponds to the electrochemically stable materials. The predicted $\Delta G_{pbx} > 0$ can be tolerated, e.g., due to high kinetic barriers of solid−solid phase transformations. Overall, the method allows one to chart electrochemical instability maps for selected (meta)stable materials, enabling quantification of thermodynamic propensity to be stable, passivate, or corrode.

A successful application of this computational methodology validated by experiments was recently carried out on the example of the Fe−V−O−H system in aqueous media.[75] By computing the relative Gibbs free energies of possible decomposition products as a function of pH and potential, thermodynamic propensity toward electrochemical stabilization, passivation, and corrosion was analyzed. Figure 4 shows the

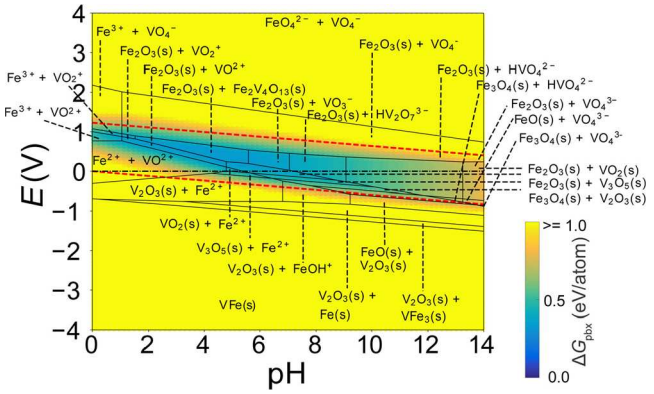

Figure 4. Computational Pourbaix diagram of the Fe−V−O−H system. The Gibbs free energy, ΔG_{pbx}, of the metastable triclinic-$FeVO_4$ phase with respect to the Pourbaix stable phases is superimposed and is represented by the color bar. The red dashed lines denote potentials of 0 and 1.23 V_{RHE}. Reprinted with permission from ref 75. Copyright 2017 American Chemical Society.

DFT computed Pourbaix diagram of the Fe−V−O−H system with a 1:1 composition of Fe and V. Thermodynamic stability regions of the relevant ground-state solids (FeO, Fe_2O_3, Fe_3O_4, $Fe_2V_2O_{13}$, Fe_3V, FeV, VO_2, V_2O_3, V_3O_4, and V_2O_5) are depicted. The metastable triclinic-$FeVO_4$ phase is not represented in this equilibrium Pourbaix diagram, as it is predicted to spontaneously decompose into stable $Fe_2V_4O_{13}$ and Fe_2O_3. However, the calculation of ΔG_{pbx} with respect to stable domains allows one to quantify the $FeVO_4$ instability against different possible combinations. The predicted ΔG_{pbx} of the metastable triclinic-$FeVO_4$ phase can be superimposed on the Pourbaix diagram, as shown in Figure 4 by the color bar. The minimum value of ΔG_{pbx} is found to be 0.34 eV/atom at pH = 1.63 and E = 1.85 V_{RHE}. In this work, the same theoretical analysis was also performed for 20 more materials, revealing that the systems with ΔG_{pbx} up to 0.5 eV/atom may remain stable in aqueous environments. When ΔG_{pbx} exceeds 0.5 eV/atom and materials exhibit decomposition to only aqueous species, materials corrosion is likely to occur. However, when decomposition to both solid and aqueous phases is possible, materials can display self-passivation.

The proposed extension of Pourbaix diagrams is certainly an advancement toward a more comprehensive thermodynamics-based analysis of material corrosion behavior. However, it should also be pointed out that in electrochemical applications the formation of an electrical double layer can modify thermodynamic stability of the considered phases, which is not captured in the discussed analysis. In addition, the employed concentration of dissolved metal ions (10^{-5} M) is quite arbitrary and may not be adequate for real systems. For example, different ions are characterized by different solubilities that also depend strongly on solution pH. In fact, the equilibrium lines can displace quite significantly relative to the ΔG_{pbx} values when other ion concentrations are considered.[7]

Kinetics of Dissolution and Surface Restructuring. Pourbaix diagrams, being purely equilibrium thermodynamics-based charts, completely ignore the kinetics of interfacial processes such as dissolution or solid−solid transformations. However, it is known that the corrosion behavior of electrochemical interfaces may be dominated by kinetics rather than thermodynamics. Unlike Pourbaix diagrams used to identify thermodynamic driving forces for materials instability, we still do not have canonical rules to enable predictions about kinetically controlled corrosion behavior.

One exemplary material is $BiVO_4$ known as one of the best-performing oxide photoanodes for water splitting.[79] This material is well suited for driving the OER because of its favorable combination of electronic-structure properties. In a recent study[80] corrosion mechanisms of $BiVO_4$ were investigated by combining experiments and DFT simulations. An in-depth analysis of compositional and morphological changes in $BiVO_4$ under photoelectrochemical water splitting conditions revealed chemical instabilities that are not predicted by the computational Pourbaix diagram involving stable solid oxide phases. In particular, Figure 5 shows the DFT computed Pourbaix diagram used to provide insight into the thermodynamic stability of $BiVO_4$. It is predicted that $BiVO_4$ should be stable in the pH range from 1 to 11, but is expected to decompose at the oxygen evolution potentials. Specifically, V should dissolve as VO_4^- ions, but the surface should self-passivate due to the formation of a chemically stable passivating bismuth-oxide film impeding $BiVO_4$ dissolution. However, the loss of both Bi and V species was experimentally detected. Importantly, while $BiVO_4$ dissolution was accelerated under illumination, it was also observed under dark conditions. These results indicate that the thermodynamic equilibrium at the solid/liquid interface is not established, suggesting kinetically inaccessible self-passivation. A recent combined experimental-theoretical study also identified kinetic origins of the metastable zone width in the Pourbaix diagram of δ'-MnO_2.[81] Therefore, computational

https://doi.org/10.1021/acs.jpcc.3c01727
J. Phys. Chem. C XXXX, XXX, XXX−XXX

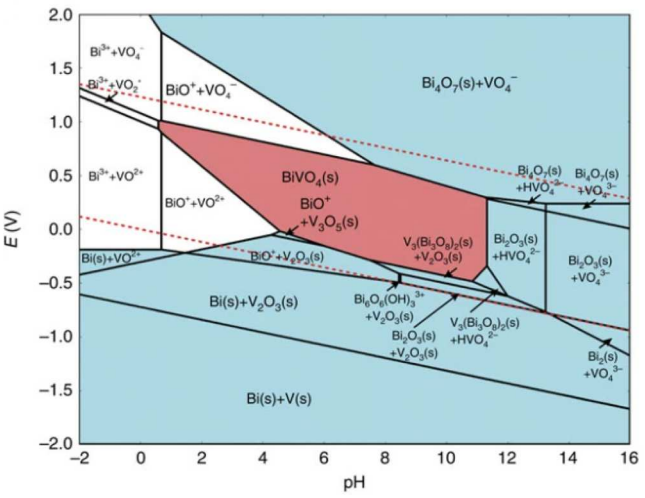

Figure 5. Computational Pourbaix diagram of the 50−50% Bi−V system in aqueous solution assuming both Bi and V ion concentrations at 10^{-5} mol kg^{-1}. Reprinted with permission from ref 80. Copyright 2016 Nature Portfolio.

investigations of possible kinetically controlled transformations are necessary for accurate descriptions of materials stability under reaction conditions.

In another investigation,[72] the OER activity and stability of Co-based perovskite catalysts with and without Fe doping was examined as a function of solution pH. It was shown that although Pourbaix diagrams of $Ba_{0.5}Sr_{0.5}CoO_{3-\delta}$ and $La_{0.2}Sr_{0.8}Co_{0.8}Fe_{0.2}O_{3-\delta}$ identified their thermodynamic instabilities at pH 13, the catalysts exhibited increased current density during the first cycles, suggesting that cation dissolution kinetics can also contribute to slowing down materials degradation.

In an attempt to provide insights into the kinetics of metal dissolution from OER-active metal oxides, a series of recent studies invoked AIMD free energy simulations.[71,82−84] In addition to the dissolution kinetics, these modeling studies also provide information about the chemistry of dissolution intermediates. Owing to the quantum-mechanical treatment of the electronic structure, AIMD methods allow one to capture the intricate changes in electronic-structure properties during the transition-metal dissolution process.

Taking rutile IrO_2 as a representative OER catalyst, Ir dissolution from the $IrO_2(110)$ surface into water solution was modeled using AIMD thermodynamic integration simulations as a function of electrode potential.[82] It was shown that Ir should dissolve as IrO_3 at high anodic potentials and as Ir^{3+} species at low potentials, going through the same surface-bound IrO_2OH dissolution intermediate that was found to be stable in a broad range of electrode potentials. This dissolution mechanism appears to be consistent with prior experiments involving dissolution measurements and the detection of the OER intermediates using online electrochemical mass spectrometry. Importantly, the dissolution kinetics estimated from simulations was found to be more favorable when proceeding through the pathway involving a higher oxidation-state intermediate (i.e., IrO_3). Figure 6 shows a determined relationship between the OER activity of dissolution intermediates and kinetic barriers of their dissolution into water as a function of the Ir oxidation state. This information is not available from the computed Pourbaix diagram of IrO_2 (Figure 6a). It should be noted, however, that this theoretical study did not consider other factors that can influence the overall dissolution kinetics such as the kinetics of IrO_3 hydrolysis, decomposition into IrO_2 and O_2, and contribution from a potential participation of the lattice oxygen in the OER. Another important aspect that is typically ignored when modeling degradation of electrochemical materials is electric-field effects. However, electric fields at electrochemical interfaces could be strong (~0.1 eV/Å) providing a substantial contribution to the overall driving force for surface restructuring and metal dissolution. We note that while the role of electric-field effects on electrocatalytic activity is now well recognized,[85,86] how these effects are manifested in electrochemical corrosion are yet to be understood.

In light of the above discussion on the corrosion of photoelectrochemical materials such as $BiVO_4$, we also want to point out that key differences exist between metal and semiconductor electrodes. It appears that Gerischer and Bard were among the first to realize the important role of two types of electronic charge carriers (from the conduction and valence bands) present in semiconductors for materials stability.[87−90] These investigations led to the formulation of a first general kinetic model of semiconductor decomposition reactions.[88] In brief, the presence of a hole will weaken the chemical bond and favor nucleophilic attack, whereas the accumulation of electrons will favor attack by electrophilic reactants. This will occur under

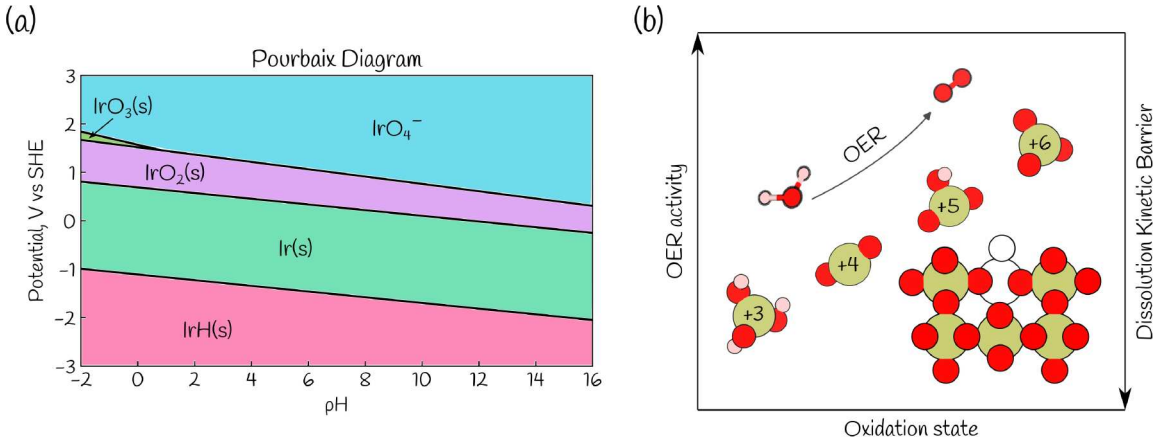

Figure 6. (a) Computational Pourbaix diagram for the Ir-aqueous system. (b) Schematic showing the relationship between the OER activity and the Ir dissolution activation barrier for Ir dissolution intermediates as a function of Ir oxidation state.

https://doi.org/10.1021/acs.jpcc.3c01727
J. Phys. Chem. C XXXX, XXX, XXX−XXX

anodic and cathodic polarization of the semiconductor electrodes, respectively. To account for the nonequilibrium illumination conditions, the concept of the nonequilibrium quasi-Fermi energy for electrons and holes in semiconductors was first introduced by Shockley for p−n junctions[91] and then adopted by Gerischer for photoelectrochemical systems.[90] Specifically, the Gerischer model of semiconductor stability states that the semiconductor−water interface is stable if the reductive potential $E(H^+/H_2)$ is more positive versus NHE than the cathodic decomposition potential of the semiconductor $E_{n,d}$(pH), and if the oxidative potential $E(O_2/H_2O)$ is more negative versus NHE than the anodic decomposition of the semiconductor $E_{p,d}$(pH). $E_{n,d}$(pH) and $E_{p,d}$(pH) are dependent on solution pH and can be obtained from either experiments or thermodynamic calculations. However, the true nonequilibrium thermodynamic theory of irreversible photoelectrochemical reactions must involve additional concepts such as the rate of entropy production and Onsager reciprocal relations.[92,93]

From the standpoint of first-principles simulations, the investigation of photoelectrochemical materials represents serious challenges. In particular, theoretical models have to provide the proper description of charge localization, mobilities, and energetics of photogenerated electrons and holes at the semiconductor−water interface. In the past few years, significant progress has been achieved in this area[94−96] including insights into charge transfer mechanisms at out-of-equilibrium conditions with the help of approaches such as AIMD simulations and nonequilibrium Green's function formalism.[97,98] Importantly, modeling studies demonstrated significant differences between the properties of bulk and surface charge carriers as the band edge positions depend strongly on the aqueous interfacial structure and chemistry.[95] Nevertheless, first-principles based understanding of corrosion mechanisms in photoelectrochemical materials remains very limited,[99,100] and future research in this direction seems particularly promising.

Finally, we also want to mention some approaches intended to extend the utility of Pourbaix diagrams by including kinetic parameters through the construction of so-called dynamic or kinetic potential−pH diagrams.[101,102] For instance, in the approach proposed by Bard[102] the extension of thermodynamic potential−pH maps is done by adding a third axis representing the rate of the investigated reaction as provided by the potential- and pH-dependent current density. In this work, the approach was demonstrated on the example of four OER-active electrocatalysts (IrO_2, Co_3O_4, Co_3O_4 electrodeposited in a phosphate medium, and Pt). This method, however, relies on the use of experimentally measured current densities as a way to represent kinetic information. It would be interesting if similar but computational thermodynamic−kinetic diagrams could be constructed.

SUMMARY AND OUTLOOK

The field of electrochemical corrosion of energy materials has flourished during the past decade, rapidly transforming from a research backwater to the mainstream. Equilibrium thermodynamics-based Pourbaix diagrams remain perhaps the most general and elegant framework to analyze driving forces of material (in)stability in aqueous media. However, the need for more accurate quantitative descriptions of reactive electrochemical interfaces under varying conditions of energy conversion calls for theoretical stability analyses beyond classical Pourbaix diagrams. Drawing on examples from (photo)electrocatalysis, in this Perspective we discussed a number of aspects that are not covered by conventional Pourbaix diagrams but are important for deeper understanding of electrochemical stability of energy conversion materials. We highlighted a few exemplary atomistic modeling studies aimed to assist experimental investigations in interrogating the effects of potentiodynamic electrode polarization, strain, interfacial electrochemical reactions, and surface reorganization as well as thermodynamics vs kinetics. We also noted some key differences in the electronic-structure properties of metallic and semiconducting electrodes that have direct implications for materials stability. Given the diversity of the factors that can influence the corrosion behavior of (photo)electrochemical materials, it seems quite challenging to come up with a universal theoretical framework.

Our objective was not to provide a comprehensive overview of the factors that might affect the electrochemical stability of energy materials. Rather, we aimed to outline just a few directions where, in our opinion, computational modeling can considerably improve the basic understanding of materials stability. We also suggest that (i) more joint theory-experiment efforts should be directed at gaining mechanistic atomic-level understanding of corroding electrochemical interfaces, (ii) machine learning approaches can play an invaluable role in complementing both experiments and *ab initio* modeling to embrace the complexity of highly dynamic electrode/electrolyte interfaces, and (iii) more activities should be devoted to developing and applying theoretical methods to investigate the instability of (photo)electrochemical interfaces triggered by nonequilibrium conditions of energy conversion.

AUTHOR INFORMATION

Corresponding Author

Vitaly Alexandrov − *Department of Chemical and Biomolecular Engineering, University of Nebraska-Lincoln, Lincoln, Nebraska 68588, United States; Nebraska Center for Materials and Nanoscience, University of Nebraska-Lincoln, Lincoln, Nebraska 68588, United States;* orcid.org/0000-0003-2063-6914; Phone: +1 (402) 472-5323; Email: valexandrov2@unl.edu; Fax: +1 (402) 472-5323

Authors

Alexandra Zagalskaya − *Department of Chemical and Biomolecular Engineering, University of Nebraska-Lincoln, Lincoln, Nebraska 68588, United States; Quantum Simulations Group, Materials Science Division, Lawrence Livermore National Laboratory, Livermore, California 94550, United States*

Payal Chaudhary − *Department of Chemical and Biomolecular Engineering, University of Nebraska-Lincoln, Lincoln, Nebraska 68588, United States*

Complete contact information is available at: https://pubs.acs.org/10.1021/acs.jpcc.3c01727

Author Contributions

§A.Z. and P.C. contributed equally to this work.

Notes

The authors declare no competing financial interest.

https://doi.org/10.1021/acs.jpcc.3c01727
J. Phys. Chem. C XXXX, XXX, XXX−XXX

Biographies

Alexandra Zagalskaya obtained her Ph.D. in Materials Engineering at the University of Nebraska-Lincoln with Prof. Vitaly Alexandrov. She is currently a postdoctoral researcher in the Quantum Simulations Group at Lawrence Livermore National Laboratory. Her area of research expertise is in the implementation and application of theoretical/modeling approaches to investigate the properties of electrochemical interfaces.

Payal Chaudhary received her M.Tech. degree in Materials Science and Technology at the Indian Institute of Technology, Varanasi, India. She is currently pursuing her Ph.D. in Chemical and Biomolecular Engineering at the University of Nebraska-Lincoln under Prof. Vitaly Alexandrov's supervision. Her research focuses on the investigation of electric double layer effects in electrocatalysis.

Vitaly Alexandrov is Richard L. McNeel Associate Professor in the Department of Chemical and Biomolecular Engineering at the University of Nebraska-Lincoln (UNL). He studied electrochemistry (Diploma) and quantum chemistry (M.S.) at St. Petersburg State University and received his Ph.D. degree from Max Planck Institute for Solid State Research in 2009. He subsequently worked as a postdoctoral researcher at the University of California at Davis, University of California at Berkeley, and Pacific Northwest National Laboratory before joining UNL as an Assistant Professor in 2015. His research focuses on theoretical/computational studies of electrochemical materials with applications in energy conversion and storage.

■ ACKNOWLEDGMENTS

We acknowledge funding support from the National Science Foundation (NSF) through the NSF CAREER award (grant no. CBET-1941204). This research used resources of the National Energy Research Scientific Computing Center, a DOE Office of Science User Facility supported by the Office of Science of the U.S. Department of Energy under contract no. DE-AC02-05CH11231 as well as the Holland Computing Center at the University of Nebraska-Lincoln.

■ REFERENCES

(1) Pourbaix, M. *Atlas of electrochemical equilibria in aqueous solutions*; Pergamon Press: Oxford, 1966.
(2) Persson, K. A.; Waldwick, B.; Lazic, P.; Ceder, G. Prediction of solid-aqueous equilibria: Scheme to combine first-principles calculations of solids with experimental aqueous states. *Phys. Rev. B* **2012**, *85*, 235438.
(3) Jain, A.; Ong, S. P.; Hautier, G.; Chen, W.; Richards, W. D.; Dacek, S.; Cholia, S.; Gunter, D.; Skinner, D.; Ceder, G.; et al. Commentary: The Materials Project: A materials genome approach to accelerating materials innovation. *APL Materials* **2013**, *1*, No. 011002.
(4) Patel, A. M.; Nørskov, J. K.; Persson, K. A.; Montoya, J. H. Efficient Pourbaix diagrams of many-element compounds. *Phys. Chem. Chem. Phys.* **2019**, *21*, 25323−25327.
(5) Hansen, H. A.; Rossmeisl, J.; Nørskov, J. K. Surface Pourbaix diagrams and oxygen reduction activity of Pt, Ag and Ni(111) surfaces studied by DFT. *Phys. Chem. Chem. Phys.* **2008**, *10*, 3722−3730.
(6) Huang, L.-F.; Scully, J. R.; Rondinelli, J. M. Modeling Corrosion with First-Principles Electrochemical Phase Diagrams. *Annu. Rev. Mater. Res.* **2019**, *49*, 53−77.
(7) Barthel, J.; Deiss, R. The limits of the Pourbaix diagram in the interpretation of the kinetics of corrosion and cathodic protection of underground pipelines. *Materials and Corrosion* **2021**, *72*, 434−445.
(8) Topalov, A. A.; Katsounaros, I.; Auinger, M.; Cherevko, S.; Meier, J. C.; Klemm, S. O.; Mayrhofer, K. J. J. Dissolution of Platinum: Limits for the Deployment of Electrochemical Energy Conversion? *Angew. Chem., Int. Ed.* **2012**, *51*, 12613−12615.
(9) Zihrul, P.; Hartung, I.; Kirsch, S.; Huebner, G.; Hasché, F.; Gasteiger, H. A. Voltage Cycling Induced Losses in Electrochemically Active Surface Area and in H2/Air-Performance of PEM Fuel Cells. *J. Electrochem. Soc.* **2016**, *163*, F492.
(10) Speck, F. D.; Zagalskaya, A.; Alexandrov, V.; Cherevko, S. Periodicity in the Electrochemical Dissolution of Transition Metals. *Angew. Chem., Int. Ed.* **2021**, *60*, 13343−13349.
(11) Duan, Z.; Henkelman, G. Atomic-Scale Mechanisms of Electrochemical Pt Dissolution. *ACS Catal.* **2021**, *11*, 14439−14447.
(12) Munarriz, J.; Zhang, Z.; Sautet, P.; Alexandrova, A. N. Graphite-Supported Pt_n Cluster Electrocatalysts: Major Change of Active Sites as a Function of the Applied Potential. *ACS Catal.* **2022**, *12*, 14517−14526.
(13) Timoshenko, J.; Bergmann, A.; Rettenmaier, C.; Herzog, A.; Arán-Ais, R. M.; Jeon, H. S.; Haase, F. T.; Hejral, U.; Grosse, P.; Kühl, S.; et al. Steering the structure and selectivity of CO_2 electroreduction catalysts by potential pulses. *Nature Catalysis* **2022**, *5*, 259−267.
(14) Klemm, S. O.; Topalov, A. A.; Laska, C. A.; Mayrhofer, K. J. Coupling of a high throughput microelectrochemical cell with online multielemental trace analysis by ICP-MS. *Electrochem. Commun.* **2011**, *13*, 1533−1535.

https://doi.org/10.1021/acs.jpcc.3c01727
J. Phys. Chem. C XXXX, XXX, XXX−XXX

(15) Senftle, T. P.; Hong, S.; Islam, M. M.; Kylasa, S. B.; Zheng, Y.; Shin, Y. K.; Junkermeier, C.; Engel-Herbert, R.; Janik, M. J.; Aktulga, H. M.; et al. The ReaxFF reactive force-field: development, applications and future directions. *npj Computational Materials* **2016**, *2*, 15011.
(16) Kirchhoff, B.; Braunwarth, L.; Jung, C.; Jónsson, H.; Fantauzzi, D.; Jacob, T. Simulations of the Oxidation and Degradation of Platinum Electrocatalysts. *Small* **2020**, *16*, 1905159.
(17) Fantauzzi, D.; Bandlow, J.; Sabo, L.; Mueller, J. E.; van Duin, A. C. T.; Jacob, T. Development of a ReaxFF potential for Pt− O systems describing the energetics and dynamics of Pt− oxide formation. *Phys. Chem. Chem. Phys.* **2014**, *16*, 23118−23133.
(18) Bang, S.; Sengul, M.; Fan, Z.; Ndayishimiye, A.; van Duin, A.; Randall, C. Morphological and chemical evolution of transient interfaces during zinc oxide cold sintering process. *Materials Today Chemistry* **2022**, *24*, 100925.
(19) Wexler, R. B.; Qiu, T.; Rappe, A. M. Automatic Prediction of Surface Phase Diagrams Using Ab Initio Grand Canonical Monte Carlo. *J. Phys. Chem. C* **2019**, *123*, 2321−2328.
(20) Lim, J. S.; Vandermause, J.; van Spronsen, M. A.; Musaelian, A.; Xie, Y.; Sun, L.; O'Connor, C. R.; Egle, T.; Molinari, N.; Florian, J.; et al. Evolution of Metastable Structures at Bimetallic Surfaces from Microscopy and Machine-Learning Molecular Dynamics. *J. Am. Chem. Soc.* **2020**, *142*, 15907−15916.
(21) Zhou, C.; Ngan, H. T.; Lim, J. S.; Darbari, Z.; Lewandowski, A.; Stacchiola, D. J.; Kozinsky, B.; Sautet, P.; Boscoboinik, J. A. Dynamical Study of Adsorbate-Induced Restructuring Kinetics in Bimetallic Catalysts Using the PdAu(111) Model System. *J. Am. Chem. Soc.* **2022**, *144*, 15132−15142.
(22) Price, C. C.; Singh, A.; Frey, N. C.; Shenoy, V. B. Efficient catalyst screening using graph neural networks to predict strain effects on adsorption energy. *Sci. Adv.* **2022**, *8*, eabq5944.
(23) Marcella, N.; Lim, J. S.; Płonka, A. M.; Yan, G.; Owen, C. J.; van der Hoeven, J. E. S.; Foucher, A. C.; Ngan, H. T.; Torrisi, S. B.; Marinkovic, N. S.; et al. Decoding reactive structures in dilute alloy catalysts. *Nat. Commun.* **2022**, *13*, 832.
(24) Zhou, Y.; Ouyang, Y.; Zhang, Y.; Li, Q.; Wang, J. Machine Learning Assisted Simulations of Electrochemical Interfaces: Recent Progress and Challenges. *J. Phys. Chem. Lett.* **2023**, *14*, 2308−2316.
(25) Galvao, T. L. P.; Novell-Leruth, G.; Kuznetsova, A.; Tedim, J.; Gomes, J. R. B. Elucidating Structure−Property Relationships in Aluminum Alloy Corrosion Inhibitors by Machine Learning. *J. Phys. Chem. C* **2020**, *124*, 5624−5635.
(26) Coelho, L. B.; Zhang, D.; Van Ingelgem, Y.; Steckelmacher, D.; Nowé, A.; Terryn, H. Reviewing machine learning of corrosion prediction in a data-oriented perspective. *npj Materials Degradation* **2022**, *6*, 8.
(27) Wang, Y.; Goh, B.; Nelaturu, P.; Duong, T.; Hassan, N.; David, R.; Moorehead, M.; Chaudhuri, S.; Creuziger, A.; Hattrick-Simpers, J.; et al. Integrated High-Throughput and Machine Learning Methods to Accelerate Discovery of Molten Salt Corrosion-Resistant Alloys. *Advanced Science* **2022**, *9*, 2200370.
(28) Noe, F.; Olsson, S.; Köhler, J.; Wu, H. Boltzmann generators: Sampling equilibrium states of many-body systems with deep learning. *Science* **2019**, *365*, eaaw1147.
(29) Bonati, L.; Piccini, G.; Parrinello, M. Deep learning the slow modes for rare events sampling. *Proc. Natl. Acad. Sci. U. S. A.* **2021**, *118*, No. e2113533118.
(30) Fuchs, T.; Drnec, J.; Calle-Vallejo, F.; Stubb, N.; Sandbeck, D. J. S.; Ruge, M.; Cherevko, S.; Harrington, D. A.; Magnussen, O. M. Structure dependency of the atomic-scale mechanisms of platinum electro-oxidation and dissolution. *Nature Catalysis* **2020**, *3*, 754−761.
(31) Qiu, Y.; Thomas, S.; Gibson, M. A.; Fraser, H. L.; Birbilis, N. Corrosion of high entropy alloys. *npj Materials Degradation* **2017**, *1*, 15.
(32) Shi, Y.; Yang, B.; Liaw, P. K. Corrosion-Resistant High-Entropy Alloys: A Review. *Metals* **2017**, *7*, 43.
(33) Zhang, S.; Zhang, X.; Jiang, G.; Zhu, H.; Guo, S.; Su, D.; Lu, G.; Sun, S. Tuning Nanoparticle Structure and Surface Strain for Catalysis Optimization. *J. Am. Chem. Soc.* **2014**, *136*, 7734−7739.
(34) Čolić, V.; Bandarenka, A. S. Pt Alloy Electrocatalysts for the Oxygen Reduction Reaction: From Model Surfaces to Nanostructured Systems. *ACS Catal.* **2016**, *6*, 5378−5385.
(35) Wang, X.; Zhu, Y.; Vasileff, A.; Jiao, Y.; Chen, S.; Song, L.; Zheng, B.; Zheng, Y.; Qiao, S.-Z. Strain Effect in Bimetallic Electrocatalysts in the Hydrogen Evolution Reaction. *ACS Energy Letters* **2018**, *3*, 1198−1204.
(36) Jansonius, R. P.; Reid, L. M.; Virca, C. N.; Berlinguette, C. P. Strain Engineering Electrocatalysts for Selective CO2 Reduction. *ACS Energy Letters* **2019**, *4*, 980−986.
(37) You, B.; Tang, M. T.; Tsai, C.; Abild-Pedersen, F.; Zheng, X.; Li, H. Enhancing Electrocatalytic Water Splitting by Strain Engineering. *Adv. Mater.* **2019**, *31*, 1807001.
(38) Yang, X.; Wang, Y.; Tong, X.; Yang, N. Strain Engineering in Electrocatalysts: Fundamentals, Progress, and Perspectives. *Adv. Energy Mater.* **2022**, *12*, 2102261.
(39) Shi, F.; Gao, W.; Shan, H.; Li, F.; Xiong, Y.; Peng, J.; Xiang, Q.; Chen, W.; Tao, P.; Song, C.; et al. Strain-Induced Corrosion Kinetics at Nanoscale Are Revealed in Liquid: Enabling Control of Corrosion Dynamics of Electrocatalysis. *Chem.* **2020**, *6*, 2257−2271.
(40) Chattot, R.; Martens, I.; Mirolo, M.; Ronovsky, M.; Russello, F.; Isern, H.; Braesch, G.; Hornberger, E.; Strasser, P.; Sibert, E.; et al. Electrochemical Strain Dynamics in Noble Metal Nanocatalysts. *J. Am. Chem. Soc.* **2021**, *143*, 17068−17078.
(41) Lewis, F. The palladium-hydrogen system: Structures near phase transition and critical points. *Int. J. Hydrogen Energy* **1995**, *20*, 587−592.
(42) Hersbach, T. J.; Koper, M. T. Cathodic corrosion: 21st century insights into a 19th century phenomenon. *Current Opinion in Electrochemistry* **2021**, *26*, 100653.
(43) Evazzade, I.; Zagalskaya, A.; Alexandrov, V. Revealing Elusive Intermediates of Platinum Cathodic Corrosion through DFT Simulations. *J. Phys. Chem. Lett.* **2022**, *13*, 3047−3052.
(44) Hanselman, S.; Calle-Vallejo, F.; Koper, M. T. M. Computational description of surface hydride phases on Pt(111) electrodes. *J. Chem. Phys.* **2023**, *158*, No. 014703.
(45) Scheler, T.; Degtyareva, O.; Marqués, M.; Guillaume, C. L.; Proctor, J. E.; Evans, S.; Gregoryanz, E. Synthesis and properties of platinum hydride. *Phys. Rev. B* **2011**, *83*, 214106.
(46) Nakamura, M.; Nakajima, Y.; Hoshi, N.; Tajiri, H.; Sakata, O. Effect of Non-Specifically Adsorbed Ions on the Surface Oxidation of Pt(111). *ChemPhysChem* **2013**, *14*, 2426−2431.
(47) Liu, Y.; Kawaguchi, T.; Pierce, M. S.; Komanicky, V.; You, H. Layering and Ordering in Electrochemical Double Layers. *J. Phys. Chem. Lett.* **2018**, *9*, 1265−1271.
(48) Chattot, R.; Le Bacq, O.; Beermann, V.; Kühl, S.; Herranz, J.; Henning, S.; Kühn, L.; Asset, T.; Guétaz, L.; Renou, G.; et al. Surface distortion as a unifying concept and descriptor in oxygen reduction reaction electrocatalysis. *Nat. Mater.* **2018**, *17*, 827−833.
(49) Yoo, J. S.; Rong, X.; Liu, Y.; Kolpak, A. M. Role of Lattice Oxygen Participation in Understanding Trends in the Oxygen Evolution Reaction on Perovskites. *ACS Catal.* **2018**, *8*, 4628−4636.
(50) Kasian, O.; Geiger, S.; Li, T.; Grote, J.-P.; Schweinar, K.; Zhang, S.; Scheu, C.; Raabe, D.; Cherevko, S.; Gault, B.; et al. Degradation of iridium oxides via oxygen evolution from the lattice: correlating atomic scale structure with reaction mechanisms. *Energy Environ. Sci.* **2019**, *12*, 3548−3555.
(51) Schweinar, K.; Gault, B.; Mouton, I.; Kasian, O. Lattice Oxygen Exchange in Rutile IrO_2 during the Oxygen Evolution Reaction. *J. Phys. Chem. Lett.* **2020**, *11*, 5008−5014.
(52) Lopes, P. P.; Strmcnik, D.; Tripkovic, D.; Connell, J. G.; Stamenkovic, V.; Markovic, N. M. Relationships between Atomic Level Surface Structure and Stability/Activity of Platinum Surface Atoms in Aqueous Environments. *ACS Catal.* **2016**, *6*, 2536−2544.
(53) Nørskov, J. K.; Rossmeisl, J.; Logadottir, A.; Lindqvist, L.; Kitchin, J. R.; Bligaard, T.; Jónsson, H. Origin of the Overpotential for Oxygen Reduction at a Fuel-Cell Cathode. *J. Phys. Chem. B* **2004**, *108*, 17886−17892.
(54) Man, I. C.; Su, H.-Y.; Calle-Vallejo, F.; Hansen, H. A.; Martínez, J. I.; Inoglu, N. G.; Kitchin, J.; Jaramillo, T. F.; Nørskov, J. K.; Rossmeisl,

https://doi.org/10.1021/acs.jpcc.3c01727
J. Phys. Chem. C XXXX, XXX, XXX−XXX

J. Universality in Oxygen Evolution Electrocatalysis on Oxide Surfaces. *ChemCatChem.* **2011**, *3*, 1159−1165.
(55) Bockris, J. O.; Otagawa, T. Mechanism of oxygen evolution on perovskites. *J. Phys. Chem.* **1983**, *87*, 2960−2971.
(56) Wohlfahrt-Mehrens, M.; Heitbaum, J. Oxygen evolution on Ru and RuO2 electrodes studied using isotope labelling and on-line mass spectrometry. *Journal of Electroanalytical Chemistry and Interfacial Electrochemistry* **1987**, *237*, 251−260.
(57) Macounova, K.; Makarova, M.; Krtil, P. Oxygen evolution on nanocrystalline RuO_2 and $Ru_{0.9}Ni_{0.1}O_{2-\delta}$ electrodes − DEMS approach to reaction mechanism determination. *Electrochem. Commun.* **2009**, *11*, 1865−1868.
(58) Binninger, T.; Mohamed, R.; Waltar, K.; Fabbri, E.; Levecque, P.; Kötz, R.; Schmidt, T. J. Thermodynamic explanation of the universal correlation between oxygen evolution activity and corrosion of oxide catalysts. *Sci. Rep.* **2015**, *5*, 12167.
(59) Grimaud, A.; Diaz-Morales, O.; Han, B.; Hong, W. T.; Lee, Y.-L.; Giordano, L.; Stoerzinger, K. A.; Koper, M. T. M.; Shao-Horn, Y. Activating lattice oxygen redox reactions in metal oxides to catalyse oxygen evolution. *Nat. Chem.* **2017**, *9*, 457−465.
(60) Fabbri, E.; Schmidt, T. J. Oxygen Evolution Reaction—The Enigma in Water Electrolysis. *ACS Catal.* **2018**, *8*, 9765−9774.
(61) Zagalskaya, A.; Alexandrov, V. Role of Defects in the Interplay between Adsorbate Evolving and Lattice Oxygen Mechanisms of the Oxygen Evolution Reaction in RuO_2 and IrO_2. *ACS Catal.* **2020**, *10*, 3650−3657.
(62) Zagalskaya, A.; Evazzade, I.; Alexandrov, V. Ab Initio Thermodynamics and Kinetics of the Lattice Oxygen Evolution Reaction in Iridium Oxides. *ACS Energy Letters* **2021**, *6*, 1124−1133.
(63) Grimaud, A.; Hong, W. T.; Shao-Horn, Y.; Tarascon, J.-M. Anionic redox processes for electrochemical devices. *Nat. Mater.* **2016**, *15*, 121−126.
(64) Zhang, N.; Xiong, Y. Lattice Oxygen Activation for Enhanced Electrochemical Oxygen Evolution. *J. Phys. Chem. C* **2023**, *127*, 2147−2159.
(65) Mefford, J. T.; Rong, X.; Abakumov, A. M.; Hardin, W. G.; Dai, S.; Kolpak, A. M.; Johnston, K. P.; Stevenson, K. J. Water electrolysis on $La_{1-x}Sr_xCoO_{3-\delta}$ perovskite electrocatalysts. *Nat. Commun.* **2016**, *7*, 11053.
(66) Wan, G.; Freeland, J. W.; Kloppenburg, J.; Petretto, G.; Nelson, J. N.; Kuo, D.-Y.; Sun, C.-J.; Wen, J.; Diulus, J. T.; Herman, G. S.; et al. Amorphization mechanism of $SrIrO_3$ electrocatalyst: How oxygen redox initiates ionic diffusion and structural reorganization. *Sci. Adv.* **2021**, *7*, eabc7323.
(67) Willsau, J.; Wolter, O.; Heitbaum, J. Does the oxide layer take part in the oxygen evolution reaction on platinum?: A DEMS study. *Journal of Electroanalytical Chemistry and Interfacial Electrochemistry* **1985**, *195*, 299−306.
(68) Stoerzinger, K. A.; Diaz-Morales, O.; Kolb, M.; Rao, R. R.; Frydendal, R.; Qiao, L.; Wang, X. R.; Halck, N. B.; Rossmeisl, J.; Hansen, H. A.; et al. Orientation-Dependent Oxygen Evolution on RuO2 without Lattice Exchange. *ACS Energy Letters* **2017**, *2*, 876−881.
(69) Liu, J.; Jia, E.; Stoerzinger, K. A.; Wang, L.; Wang, Y.; Yang, Z.; Shen, D.; Engelhard, M. H.; Bowden, M. E.; Zhu, Z.; et al. Dynamic Lattice Oxygen Participation on Perovskite $LaNiO_3$ during Oxygen Evolution Reaction. *J. Phys. Chem. C* **2020**, *124*, 15386−15390.
(70) Czioska, S.; Boubnov, A.; Escalera-López, D.; Geppert, J.; Zagalskaya, A.; Röse, P.; Saraçi, E.; Alexandrov, V.; Krewer, U.; Cherevko, S.; et al. Increased Ir−Ir Interaction in Iridium Oxide during the Oxygen Evolution Reaction at High Potentials Probed by Operando Spectroscopy. *ACS Catal.* **2021**, *11*, 10043−10057.
(71) Evazzade, I.; Zagalskaya, A.; Alexandrov, V. On the Role of Interfacial Water Dynamics for Electrochemical Stability of RuO_2 and IrO_2. *ChemCatChem.* **2022**, *14*, No. e202200932.
(72) Kim, B.-J.; Fabbri, E.; Borlaf, M.; Abbott, D. F.; Castelli, I. E.; Nachtegaal, M.; Graule, T.; Schmidt, T. J. Oxygen evolution reaction activity and underlying mechanism of perovskite electrocatalysts at different pH. *Mater. Adv.* **2021**, *2*, 345−355.
(73) Fabbri, E.; Nachtegaal, M.; Binninger, T.; Cheng, X.; Kim, B.-J.; Durst, J.; Bozza, F.; Graule, T.; Schäublin, R.; Wiles, L.; et al. Dynamic surface self-reconstruction is the key of highly active perovskite nano-electrocatalysts for water splitting. *Nat. Mater.* **2017**, *16*, 925−931.
(74) Chung, D. Y.; Lopes, P. P.; Farinazzo Bergamo Dias Martins, P.; He, H.; Kawaguchi, T.; Zapol, P.; You, H.; Tripkovic, D.; Strmcnik, D.; Zhu, Y.; et al. Dynamic stability of active sites in hydr(oxy)oxides for the oxygen evolution reaction. *Nat. Energy* **2020**, *5*, 222−230.
(75) Singh, A. K.; Zhou, L.; Shinde, A.; Suram, S. K.; Montoya, J. H.; Winston, D.; Gregoire, J. M.; Persson, K. A. Electrochemical Stability of Metastable Materials. *Chem. Mater.* **2017**, *29*, 10159−10167.
(76) Shao, Q.; Wang, Y.; Yang, S.; Lu, K.; Zhang, Y.; Tang, C.; Song, J.; Feng, Y.; Xiong, L.; Peng, Y.; et al. Stabilizing and Activating Metastable Nickel Nanocrystals for Highly Efficient Hydrogen Evolution Electrocatalysis. *ACS Nano* **2018**, *12*, 11625−11631.
(77) Poths, P.; Alexandrova, A. N. Theoretical Perspective on Operando Spectroscopy of Fluxional Nanocatalysts. *J. Phys. Chem. Lett.* **2022**, *13*, 4321−4334.
(78) Jin, H.; Song, T.; Paik, U.; Qiao, S.-Z. Metastable Two-Dimensional Materials for Electrocatalytic Energy Conversions. *Accounts of Materials Research* **2021**, *2*, 559−573.
(79) Park, Y.; McDonald, K. J.; Choi, K.-S. Progress in bismuth vanadate photoanodes for use in solar water oxidation. *Chem. Soc. Rev.* **2013**, *42*, 2321−2337.
(80) Toma, F. M.; Cooper, J. K.; Kunzelmann, V.; McDowell, M. T.; Yu, J.; Larson, D. M.; Borys, N. J.; Abelyan, C.; Beeman, J. W.; Yu, K. M.; et al. Mechanistic insights into chemical and photochemical transformations of bismuth vanadate photoanodes. *Nat. Commun.* **2016**, *7*, 12012.
(81) Chen, B.-R.; Sun, W.; Kitchaev, D. A.; Stone, K. H.; Davis, R. C.; Ceder, G.; Schelhas, L. T.; Toney, M. F. Kinetic origins of the metastable zone width in the manganese oxide Pourbaix diagram. *J. Mater. Chem. A* **2021**, *9*, 7857−7867.
(82) Zagalskaya, A.; Alexandrov, V. Mechanistic Study of IrO_2 Dissolution during the Electrocatalytic Oxygen Evolution Reaction. *J. Phys. Chem. Lett.* **2020**, *11*, 2695−2700.
(83) Klyukin, K.; Zagalskaya, A.; Alexandrov, V. Role of Dissolution Intermediates in Promoting Oxygen Evolution Reaction at RuO_2(110) Surface. *J. Phys. Chem. C* **2019**, *123*, 22151−22157.
(84) Raman, A. S.; Vojvodic, A. Providing Atomistic Insights into the Dissolution of Rutile Oxides in Electrocatalytic Water Splitting. *J. Phys. Chem. C* **2022**, *126*, 922−932.
(85) Chen, L. D.; Urushihara, M.; Chan, K.; Norskov, J. K. Electric Field Effects in Electrochemical CO_2 Reduction. *ACS Catal.* **2016**, *6*, 7133−7139.
(86) Che, F.; Gray, J. T.; Ha, S.; Kruse, N.; Scott, S. L.; McEwen, J.-S. Elucidating the Roles of Electric Fields in Catalysis: A Perspective. *ACS Catal.* **2018**, *8*, 5153−5174.
(87) Beck, F.; Gerischer, H. Zum Mechanismus der anodischen Auflösung von Germanium in alkalischer Lösung. *Zeitschrift für Elektrochemie, Berichte der Bunsengesellschaft für physikalische Chemie* **1959**, *63*, 500−510.
(88) Gerischer, H.; Mindt, W. The mechanisms of the decomposition of semiconductors by electrochemical oxidation and reduction. *Electrochim. Acta* **1968**, *13*, 1329−1341.
(89) Bard, A. J.; Wrighton, M. S. Thermodynamic Potential for the Anodic Dissolution of n-Type Semiconductors: A Crucial Factor Controlling Durability and Efficiency in Photoelectrochemical Cells and an Important Criterion in the Selection of New Electrode/Electrolyte Systems. *J. Electrochem. Soc.* **1977**, *124*, 1706.
(90) Gerischer, H. Electrolytic decomposition and photodecomposition of compound semiconductors in contact with electrolytes. *J. Vac. Sci. Technol.* **1978**, *15*, 1422−1428.
(91) Shockley, W. The Theory of p-n Junctions in Semiconductors and p-n Junction Transistors. *Bell System Technical Journal* **1949**, *28*, 435−489.
(92) Salvador, P. Semiconductors' Photoelectrochemistry: A Kinetic and Thermodynamic Analysis in the Light of Equilibrium and Nonequilibrium Models. *J. Phys. Chem. B* **2001**, *105*, 6128−6141.

https://doi.org/10.1021/acs.jpcc.3c01727
J. Phys. Chem. C XXXX, XXX, XXX−XXX

(93) Bazant, M. Z. Theory of Chemical Kinetics and Charge Transfer based on Nonequilibrium Thermodynamics. *Acc. Chem. Res.* **2013**, *46*, 1144−1160.
(94) Pham, T. A.; Ping, Y.; Galli, G. Modelling heterogeneous interfaces for solar water splitting. *Nat. Mater.* **2017**, *16*, 401−408.
(95) Wiktor, J.; Pasquarello, A. Electron and Hole Polarons at the $BiVO_4$ − Water Interface. *ACS Appl. Mater. Interfaces* **2019**, *11*, 18423−18426.
(96) Lyu, S.; Wiktor, J.; Pasquarello, A. Oxygen Evolution at the $BiVO_4$ − Water Interface: Mechanism of the Water Dehydrogenation Reaction. *ACS Catal.* **2022**, *12*, 11734−11742.
(97) Akimov, A. V.; Neukirch, A. J.; Prezhdo, O. V. Theoretical Insights into Photoinduced Charge Transfer and Catalysis at Oxide Interfaces. *Chem. Rev.* **2013**, *113*, 4496−4565.
(98) Ding, Z.; Goldsmith, Z. K.; Selloni, A. Pathways for Electron Transfer at MgO Water Interfaces from Ab Initio Molecular Dynamics. *J. Am. Chem. Soc.* **2022**, *144*, 2002−2009.
(99) Mosconi, E.; Azpiroz, J. M.; De Angelis, F. Ab Initio Molecular Dynamics Simulations of Methylammonium Lead Iodide Perovskite Degradation by Water. *Chem. Mater.* **2015**, *27*, 4885−4892.
(100) Kaiser, W.; Ricciarelli, D.; Mosconi, E.; Alothman, A. A.; Ambrosio, F.; De Angelis, F. Stability of Tin- versus Lead-Halide Perovskites: Ab Initio Molecular Dynamics Simulations of Perovskite/Water Interfaces. *J. Phys. Chem. Lett.* **2022**, *13*, 2321−2329.
(101) Macdonald, D. D. On the Existence of Our Metals-Based Civilization: I. Phase-Space Analysis. *J. Electrochem. Soc.* **2006**, *153*, B213.
(102) Minguzzi, A.; Fan, F.-R. F.; Vertova, A.; Rondinini, S.; Bard, A. J. Dynamic potential−pH diagrams application to electrocatalysts for water oxidation. *Chem. Sci.* **2012**, *3*, 217−229.

https://doi.org/10.1021/acs.jpcc.3c01727
J. Phys. Chem. C XXXX, XXX, XXX−XXX